EXPERIMENTAL STUDY ON THE BOND BEHAVIOR BETWEEN SHEAR-STRENGTHENING FRP AND CONCRETE

P.Y. Zhou [1], G.M. Chen [1,*], W.N. Liu [1], Z.H. Tang[1], B.W. Xie[1], X.C. Liu[1] and J.F. Chen[2, 1]

[1] School of Civil and Transportation Engineering, Guangdong University of Technology, Guangzhou, 510006, China
Email: hustcgm@gdut.edu.cn (Corresponding author)

[2] School of Planning, Architecture and Civil Engineering, Queen's University Belfast, North Ireland, UK
Email: j.chen@qub.ac.uk

Keywords: FRP, Bond interface, Shear-strengthening, Debonding, Fiber tensile angle

ABSTRACT

In this study, 20 small beams with a cast-in through-crack were tested with FRP strips bonded to the beam sides to study the bond behavior between shear-strengthening FRP and concrete (referred to as "the interface" hereafter).The studied parameters included the bond length, FRP strip width and the angle between the fiber and crack (referred to as "fiber angle" hereafter) on the bond behavior of the interface. The test results show that the bond length, FRP width and the fiber angle have significant effects on the behavior of the FRP-to-concrete bond interface. The test results also indicated that the differential opening of the crack gives rise to differential stretching of FRP fibers across the FRP width, leading to non-uniform distribution of FRP strain and progressive debonding of FRP across its width.

1 INTRODUCTION

Externally bonding (EB) fiber reinforced polymer (FRP) composites to the surfaces of RC structure has become a widely adopted structural strengthening method in the past decade and shear strengthening of RC beam using EB FRP is one of such applications [1]. When EB FRP was used for shear strengthening of RC beams, one of the following strengthening configurations is usually adopted: full wraps, U-wraps and FRP side strips [2]. Existing studies have shown that the vast majority of beams strengthened using FRP U-wrap and all those strengthened with side strips fail by FRP debonding. In existing strength models and design provisions, it is a common to use the bond strength models deduced based on the experimental data of FRP-to-concrete bonded joints (e.g. single-shear test or double-shear test) to determine the shear contribution of FRP for the FRP debonding (e.g. [2]). However, the stress states of the FRP-to-concrete bonded interfaces in FRP shear-strengthened RC beams are quite different from those in single- or double-shear test. The shear strength models deduced based on the test data of the FRP-to-concrete bonded joints may overestimate the shear contribution of FRP, leading to unsafe results. Against this background, in this study, 20 small beam specimens with a cast-in through-crack were tested with FRP strips bonded to their sides to study the bond behavior between the shear-strengthening FRP and concrete. The test results showed that the maximum strain in shear-strengthened FRP is affected significantly by several factors including the fiber angle. The test results obtained in the present study provide a basis for further study on the shear strength of FRP shear-strengthened beams.

2 EXPERIMENTAL PROGRAM

A total of 20 beam specimens were tested in which the effects of three parameters, including the bond length, FRP width and fiber angle on the bond behavior were investigated. Details of the specimens are shown in Table 1. The designations of specimens begin with the letter "B" (for "beam"); followed by a number representing the bond length of FRP; then the number of FRP layers; the FRP strip width; and finally the fiber angle.

Table 1 Details of small beam specimens.

Test beam	Bond length L_f（mm）	Thickness of FRP sheet t_f（mm）	Strip width w_f（mm）	Fiber angle θ（°）
B60-1-50-45	60	0.167	50	45
B90-1-50-45	90	0.167	50	45
B120-1-50-45	120	0.167	50	45
B150-1-50-45	150	0.167	50	45
B120-1-25-45	120	0.167	25	45
B120-1-75-45	120	0.167	75	45
B120-1-50-0	120	0.167	50	0
B120-1-50-15	120	0.167	50	15
B120-1-50-30	120	0.167	50	30
B120-1-50-60	120	0.167	50	60
B60-2-50-45	60	0.334	50	45
B90-2-50-45	90	0.334	50	45
B120-2-50-45	120	0.334	50	45
B150-2-50-45	150	0.334	50	45
B120-2-25-45	120	0.334	25	45
B120-2-75-45	120	0.334	75	45
B120-2-50-0	120	0.334	50	0
B120-2-50-15	120	0.334	50	15
B120-2-50-30	120	0.334	50	30
B120-2-50-60	120	0.334	50	60

Figure 1 presents the details of the test specimens, following the design of Chen et al. [3]. The length of the test beams was 1000mm and the cross section was 100mm×250mm. The test beam consisted of two concrete blocks separated by the cast-in through crack, connected in the compression zone by two 12mm-diameter deformed steel bars.

The steel bars extruded 25mm from the two ends of the beams for the convenience of handling. The concrete had an average cylinder compressive strength of 41.7MPa at the time of beam testing. The tensile strength, modulus of elasticity, and nominal thickness of the CFRP strip were 4406MPa, 211 GPa and 0.167mm, respectively.

The tests were conducted under four-point bending with the test set-up shown in Figure 2. The specimens were loaded by a hydraulic loading system at a loading rate of 1.5kN~3kN per minute. The strain distribution in FRP strips were measured by strain gauges in 3 rows (see Fig. 1). The applied load was measured by two load cells. A LVDT was installed at the mid-span of the beam to measure the deflection. The crack opening width of the cast-in crack was measured by a crack width meter.

3 TEST RESULTS AND DISCUSSIONS

3.1 Failure mode

All the 20 test beams failed by FRP debonding. The typical failure mode is shown in Figure 3. The debonding was initiated at the intersection of the lower edge of the FRP strip and the cast-in through-crack. As the load continued to increase, the debonding propagated from the lower edge towards the upper edge and FRP debonding also propagated gradually from the cast-in through-crack to the end of the FRP strip. Eventually complete FRP debonding failure occurred accompanied by the clear sounds at the ultimate debonding failure. A thin layer of concrete was attached to the debonded surface of the

FRP strip after debonding failure, which indicates that the debonding failure occurred in the concrete adjacent to the bond interface.

3.2 FRP strain distribution

As mentioned above, three rows of strain gauges were bonded in the fiber direction to measure the strain distribution in the FRP strip. The FRP strain distribution were plotted in a 3-D coordinate system in which the X, Y axes represent the locations of strain gauges and the Z axis represents the strain value. A typical FRP strain distribution (for beam B120-1-50-45) is shown in Figure 4. It can be seen from Fig. 4 that the FRP strain distribution is nonlinear in both the fiber direction and the FRP width direction. In FRP width direction, the strain at the lower edge of the FRP strip is substantially higher than that at the upper edge at different load levels. In the fiber direction, the strain distribution is nearly symmetrical about the centerline of FRP strip in the early stages of loading, while at later stages the strain in the upper part is apparently higher than the corresponding location in the lower part, suggesting that the FRP debonding initiates at the location where the crack width is maximum and then propagates in two directions: to the upper edge of FRP strip in the FRP width direction and to the upper end of FRP strip in the fiber direction.

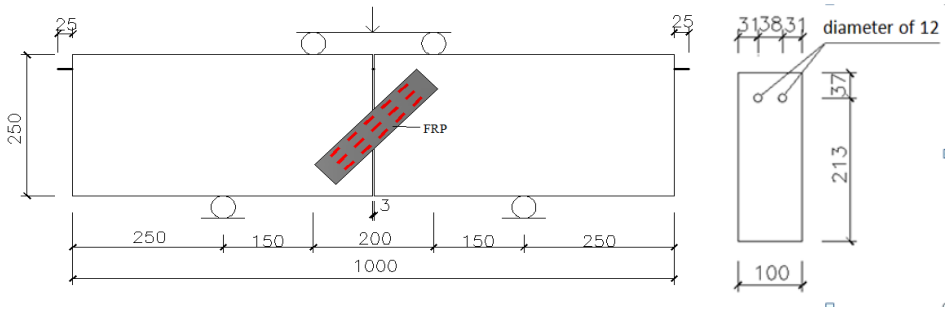

（a）Front view （b）Lateral view

Figure 1 Details of small beam specimens

Figure 2 Test set-up

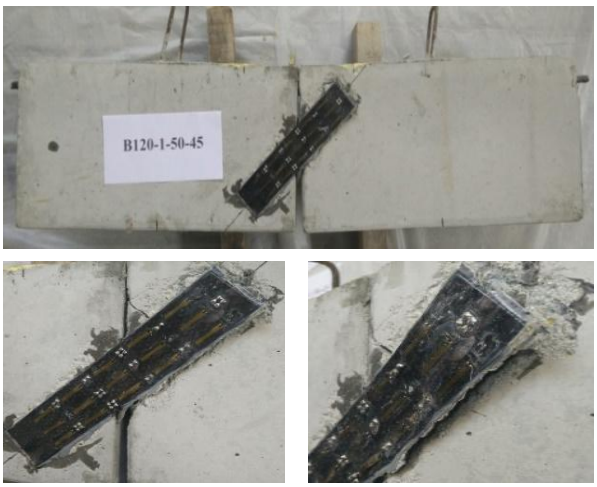

B120-1-50-45

Figure 3 Typical failure mode

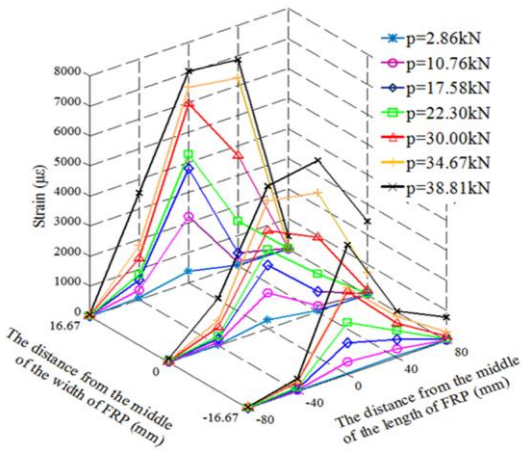

Figure 4 Typical FRP strain distribution

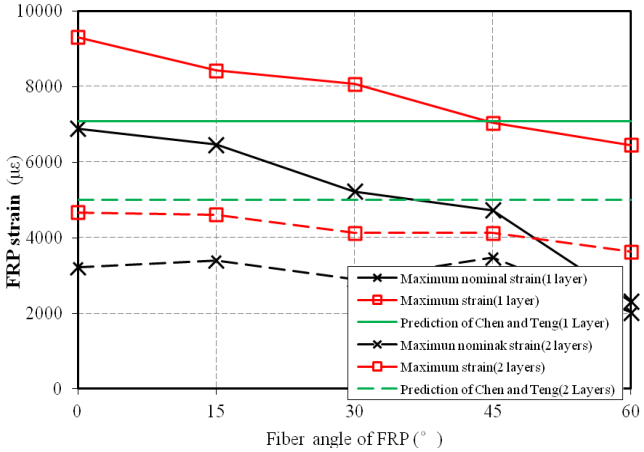

Figure 5 Effect of fiber angle on FRP strain

3.3 Effect of fiber angle, strip width and bond length on maximum FRP debonding strain

Based on the measured FRP strain data, the effects of fiber angle, strip width and bond length have been analyzed and the details can be found in Chen et al. [4]. Due to space limitation, only the effect of fiber angle is shown in Fig. 5 in which results of two FRP strips with 1 and 2 layers (i.e. specimens B120-1-50-45 and B120-2-50-45) are presented. Here the maximum nominal strain is defined as the maximum FRP strain recorded at the center of the FRP strips (i.e. at the intersection of the FRP strip middle line and the cast-in crack) on both sides. The maximum FRP strain is the maximum FRP strain recorded by all strain gauges with FRP strips on both sides of the small beam considered. From Fig. 5 it can be seen that the maximum nominal FRP strain and maximum FRP strain for both cases have an apparent trend to reduce as the FRP angle θ increases, with the maximum values being the largest when θ is 0^o. For example, when $\theta=0^o$ the maximum nominal FRP strain and maximum FRP strain for the 1-layer FRP case are 6888με and 9305με respectively, and those for the 2-layer FRP case are respectively 3225με and 4676με; when $\theta=60^o$, these strains are reduced to 2314 and 6456 for 1 layer FRP and 2024 and 3627 for 2-layer FRP, respectively. Fig. 5 also shows that the maximum nominal strains in FRP, which may be regarded as an approximation to the average maximum strains across the FRP width, are generally significantly lower than the strain predicted by Chen and Teng's bond strength model [5] (which is only valid for the case of θ=0) although the maximum strain in FRP may be larger than that predicted by the Chen and Teng's model in some cases (e.g. $\theta \leq 45^o$ for 1-layer FRP, see Fig. 5). This clearly shows that the maximum strain and maximum nominal strain in shear-strengthening FRP can be significantly different from the maximum FRP debonding strain obtained from FRP-to-concrete bonded joint tests (e.g. single-shear or double shear tests). The direct application of bond strength models developed based on the direct shear test data may thus over-estimate the FRP shear contribution in RC beams shear strengthened with FRP.

3.4 FRP strain development: strain gauge measurement vs. PIV measurement

Fig. 7 compares the FRP strain development curves obtained from strain gauge and PIV [6-7] technique as shown in Fig. 6. It can be seen that the results from the two methods are in close agreement. An added advantage of the PIV technique is that it can continue to work to the end while strain gauges may be broken or debonded from the FRP at a high strain, as demonstrated in [4].

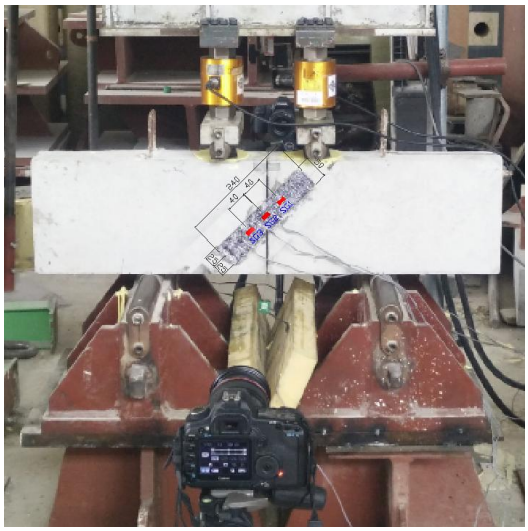

Figure 6 PIV images acquisition system (unit: mm)

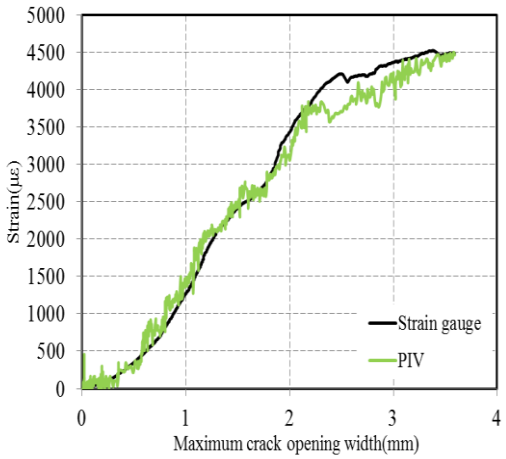

Figure 7 Strain gauge vs. PIV measurement results (at the location of strain gauge SG1 in Fig.6)

4 CONCLUSIONS

This paper has presented an experimental study on the bond behavior of shear-strengthening FRP and concrete. From the test data, comparisons and discussions presented in this paper, the following conclusions can be drawn:

1. In the shear-strengthening FRP strip, FRP debonding initiates at the location where the crack opening is largest (i.e. the intersection of the cast-in crack and the lower edge of the FRP strip) and propagates in both fiber direction and FRP width direction.

2. The strain distributions in both fiber direction and FRP width direction are nonlinear , mainly due to the differential stretching of the fibers in FRP caused by the differential crack opening along the FRP width.

3. When the fibre angle is large, both the maximum strain and the maximum nominal strain in the FRP strip are usually lower than the maximum strain predicted by the Chen and Teng's bond strength model [4] which was developed based on test data of FRP-to-concrete bonded joints (single and double-shear tests) and this only valid for the case of fibre angle equal to 0.

4. The PIV technique can provide accurate and reliable measurements on the strain in shear-strengthening FRP and can be used in further studies on RC beams shear-strengthened with EB FRP.

ACKNOWLEDGEMENTS

The authors acknowledge the financial support received from the National Natural Science Foundation of China (Project Nos. 51108097 and 51378130), Guangdong Natural Science Foundation (Project No. S2013010013293), the Department of Education of Guangdong Province for the program of Excellent Young College Teacher of Guangdong Province (Project No. Yq2013056) and the Undergraduate Training Programs for Innovation and Entrepreneurship (Project No. yj201411845094). They would also like to thank Professor Andy Take at Queen's University, Canada, for providing the PIV data-processing software. The corresponding author would like to thank the China Scholarship Council (CSC) for the scholarship awarded to him as a visiting scholar (File No. 201408440320) in the Department of Civil and Environmental Engineering, University of California, Berkeley, USA.

REFERENCES

[1] J.G. Teng, J.F. Chen, S.T. Smith and L. Lam (2002). FRP-Strengthened RC Structures, John Wiley and Sons, Inc., UK.

[2] J.F. Chen, J.G. Teng, Shear capacity of FRP-strengthened RC beams: fiber reinforced polymer rupture, Journal of Structural Engineering, ASCE, 2003, 129(5): 615-625.
[3] J.F. Chen, X.Q. Li, Y. Lu, I.M. May, T.J. Stratford, R. O'Sullivan, A. Sheil, A new test method for FRP-to-concrete bond behaviour under impact loading, 2012, Proceedings of the 12th International Symposium on Structural Engineering (ISSE-12), 17-19 November, Wuhan, China, Science Press, Beijing, 1:53-60.
[4] G.M. Chen, P.Y. Zhou, W.N. Liu, J.F. Chen, Bond behavior between shear-strengthening FRP and concrete, in preparation.
[5] J.F. Chen, J.G. Teng, Anchorage strength models for FRP and steel plates bonded to concrete, Journal of Structural Engineering, ASCE, 2001, 127(7):784-791.
[6] J. Westerweel, Fundamentals of digital particle image velocimetry, Measurement Science and Technology, 1997, 8(12): 1379-1392.
[7] D.J. White, W.A. Take, M.D. Bolton, Soil deformation measurement using particle image velocimetry (PIV) and photogrammetry, Géotechnique, 2003, 53(7): 619 –631.